

Casimir-like force between intruders in granular gases

M. Reza Shaebani

Department of Theoretical Physics, Budapest University of Technology and Economics, H-1111 Budapest, Hungary
Institute for Advanced Studies in Basic Sciences, Zanjan 45195-1159, Iran
E-mail: shaebani@comphys.uni-duisburg.de

Jalal Sarabadani

Department of Physics, University of Isfahan, Isfahan 81746, Iran
Institute for Studies in Theoretical Physics and Mathematics, Tehran 19395-5531, Iran
E-mail: j.sarabadani@phys.ui.ac.ir

Abstract. We numerically study a two-dimensional granular gas of rigid disks where an external driving force is applied to each particle in such a way that the system is driven into a steady state by balancing the energy input and the dissipation due to inelastic collisions. Two intruder particles embedded in this correlated medium experience a fluctuation-induced force – that is itself a fluctuating quantity – due to the confinement of the hydrodynamic fluctuations between them. We find that the probability distribution of this force is a Gaussian centered on a value that is proportional to the steady-state temperature and grows logarithmically with system size. We investigate the effect of the other relevant parameters and estimate the force using the Fourier transform of the fluctuating hydrodynamic fields.

PACS numbers: 45.70.Mg, 05.40.-a

Keywords: granular matter, fluctuations (theory), hydrodynamic fluctuations, stochastic processes (theory)

1. Introduction

The *Casimir force* predicted in the seminal work of Casimir [1] is an attractive force $F = -\pi^2\hbar cA/(240D^4)$ between two perfect conducting neutral plates with area A facing each other at a distance D . This attraction originates from the modification of the long-range fluctuations of the quantum electromagnetic field, due to the boundary conditions imposed by the conducting plates [2, 3, 4, 5]. The Casimir energy – the difference between the energies of the quantum electromagnetic field for the plates at distance D and at $D \rightarrow \infty$, respectively – is proportional to \hbar [1, 2, 3]; so is the Casimir force, that is the derivative of this energy with respect to the distance between the plates.

Although the original Casimir interaction has a quantum nature, such an effect occurs in many classical systems where fluctuations are of thermal origin [2]. In fact, fluctuation-induced forces appear in systems with fluctuating long-range correlations that are geometrically confined by inserting external objects in the correlated medium. Examples can be found in nematic liquid crystals [6], critical mixtures [7, 8], superfluid films [9], and granular media [10, 11, 12]. In a thermally noisy correlated medium, where long range spatial correlations exist due to thermal fluctuations, the Casimir energy (and force) is expected to be proportional to $k_B T$ [2]. The results of a recent experimental study on the critical mixtures reveal that the Casimir energy is indeed very sensitive to the temperature of the system [13]. Depending on the characteristics of the system, the fluctuation-induced force has been found to be even repulsive, e.g. in dielectric materials with nontrivial magnetic susceptibility [14], or the interaction between a perfectly conducting and an infinitely permeable plate [15].

The fluctuation-induced force between two intruder objects immersed in a granular gas is studied in [10], where it is found that the confinement of the fluctuation spectrum of the hydrodynamic pressure field induced by the intruders, leads to different local pressures in the gap between the intruders and the outside region. This effect causes an effective Casimir-like force between the intruders. The results of some experiments on granular fluids have confirmed the idea that the presence of large intruder particles modifies the thermodynamic properties such as pressure, velocity and density in the regions between the larger particles [16, 17, 18]. Appearance of long-range interactions (despite the short-range nature of the interactions on the grain scale) may shed new light on the mechanism of some collective behaviors, e.g. segregation [17, 18], in granular media.

In this paper we present the results of extensive numerical simulations to study the fluctuation-induced force between two large objects immersed in a noisy granular gas. Although the interactions between particles in granular systems are dissipative [19], we maintain the dynamics by means of an external driving force. Our main aims in the present work are to investigate the probability distribution of the fluctuating Casimir-like force and the relationship between the average force and important parameters of the system such as the steady-state temperature, the mass density of gas particles and the distance between the intruders. The question of whether the average force depends

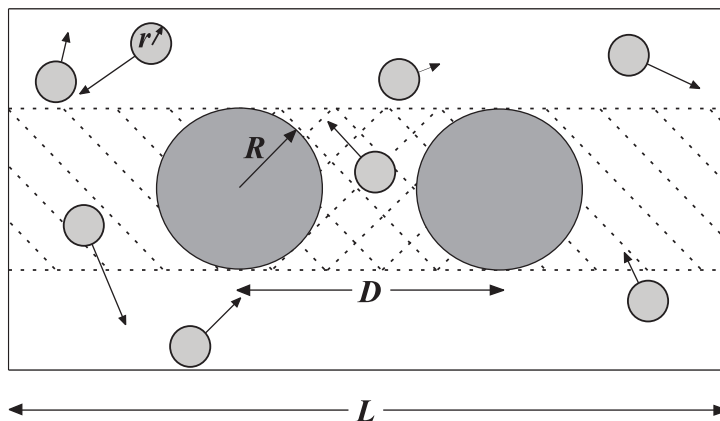


Figure 1. Schematic picture showing the simulation cell. The pressure difference between the hatched and cross-hatched regions leads to an effective repulsive force between the two intruders. We choose $L_0/r_0 = 200$, $D_0/r_0 = 30$ and $R_0/r_0 = 10$ in the reference system.

on the system size is also addressed.

2. Simulation Method

The system we consider is a two-dimensional granular gas of identical rigid disks of radius r and mass m interacting via inelastic collisions. In order to exclude the undesired effects of side walls, periodic boundary conditions are applied in both directions of the square-shaped system of length L . Two immobile rigid intruder particles of radius R and infinite mass and moment of inertia are immersed in the granular gas bed, separated by a distance D . We have one reference system whose parameters are denoted by zero subscripts (see Fig. 1). Throughout the paper we either use this reference system or vary only one parameter to check its effect while other parameters are kept fixed at their reference values. We perform molecular dynamics simulations in which the number density n of the granular gas is $0.075r^{-2}$ and the effective normal coefficient of restitution α of the particle-particle and particle-intruder collisions is set to 0.8.

The system is coupled to an external heat bath that homogeneously transfers energy into the system. The acceleration of each particle \mathbf{a}_i is perturbed instantaneously according to $\mathbf{a}'_i = \mathbf{a}_i + \boldsymbol{\xi}_i$, where prime refers to the acceleration after perturbation, and $\boldsymbol{\xi}_i$ can be considered as Gaussian white noise with zero mean and correlation $\langle \xi_{i\alpha}(t)\xi_{j\beta}(t') \rangle = \xi_0^2 \delta_{ij} \delta_{\alpha\beta} \delta(t-t')$, where α and β denote Cartesian components of vectors [20, 21]. Practically, the energy is transferred into the system in the following way [10, 20]: we update the momentum of each grain at each time step Δt . The components of the momentum are updated by adding random values that are chosen from a Gaussian distribution with zero mean and variance σ_0^2 .

3. Results

The simulation results [solid line in Fig. 2(a)] reveal that the temperature T is time dependent and finally saturates. Note that the temperature T is a uniform field in our simulations in contrast to the case where energy flows into the system from the boundaries which leads to the spatial gradient of temperature [22]. We follow a mean-field approach to describe the time evolution of T . On the one hand the system gains energy due to coupling with the heat bath. The rate of the energy gain of a single particle averaged over the uncorrelated noise source $g(\xi)$ is

$$\partial_t E = \lim_{\Delta t \rightarrow 0} \frac{1}{\Delta t} \int_{\xi} [E_i(t + \Delta t) - E_i(t)] g(\xi) d\xi = dm\xi_0^2. \quad (1)$$

On the other hand the system losses energy due to inelastic collisions. The rate of the energy loss of a single particle is described by $\partial_t E = -(1 - \alpha^2)\omega T/d = \beta T^{3/2}$ [23, 24], where d is the dimension of the system, $\omega(\propto \sqrt{T})$ is the temperature-dependent collision frequency given by the Enskog theory [25], and β is a coefficient that contains all of the relevant parameters except the temperature. Therefore the time dependence of temperature (energy) according to mean-field approximation is given by $dT/dt = -\beta T^{3/2} + dm\xi_0^2$. By integrating the equation $dT/(-\beta T^{3/2} + dm\xi_0^2) = dt$ [26], one arrives at the following expression for the evolution of T [dash-dot line in Fig. 2(a)]:

$$f(T) - f(T_i) = -dm\xi_0^2 t / 2T_{MF}, \quad (2)$$

where T_i is the initial temperature and

$$f(x) = \frac{1}{6} \ln \frac{1 - 2\sqrt{x/T_{MF}} + x/T_{MF}}{1 + \sqrt{x/T_{MF}} + x/T_{MF}} + \frac{1}{\sqrt{3}} \arctan \frac{2\sqrt{x/T_{MF}} + 1}{\sqrt{3}}. \quad (3)$$

Starting from any initial configuration, the driven granular gas finally converges to a nonequilibrium steady state, where energy dissipation due to inelastic collisions is balanced with the energy input. Although the mean-field prediction for the saturated temperature is $T_{MF} = (dm\xi_0^2/\beta)^{2/3}$, the temperature of the nonequilibrium steady state T_{NESS} [dashed line in Fig. 2(a)] is expected to be larger than T_{MF} since it is logarithmically divergent in the system size (in 2D) due to the existence of spatial hydrodynamic fluctuations [20].

After the system achieves the stationary state, we study the effective interaction between the two fixed intruders. We measure the total momenta \mathbf{P}_ℓ and \mathbf{P}_r transferred from the granular gas to the left and right intruders respectively, during a time interval τ . τ corresponds to 10^4 time steps (~ 100 collisions per grain). The components of \mathbf{P}_ℓ and \mathbf{P}_r parallel to the line connecting the two centers of intruders provide the fluctuation-induced force as $F = (P_{xr} - P_{x\ell})/2\tau$. Since this force is itself a fluctuating quantity, as expected for such correlated media [27], we let the simulation run until we measure the force for more than 10^4 consecutive time intervals τ . Figure 2(b) displays the fluctuating nature of F when measured in the steady state of the reference system. The probability distribution of F is plotted in Fig. 2(c), where it turns out that the distribution can be well fitted to a Gaussian with the standard deviation $0.612T_{MF}/r_0$. The ensemble

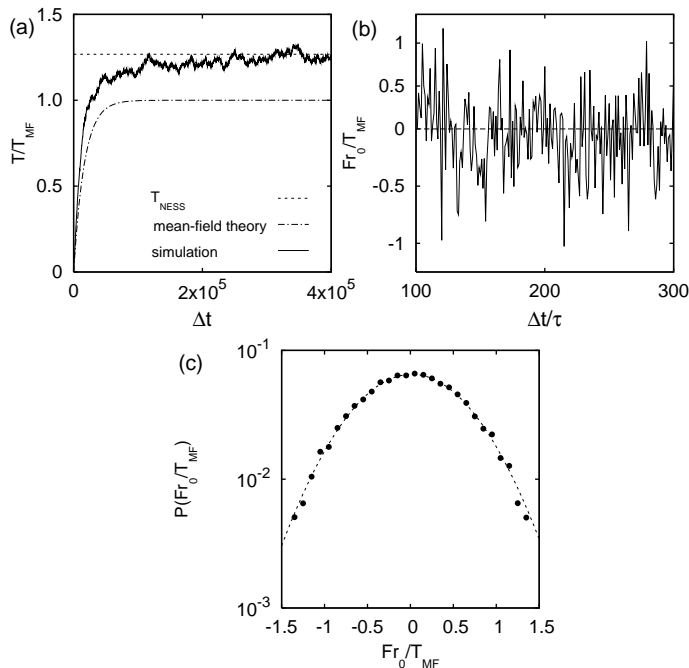


Figure 2. (a) Temperature saturation starting from a random initial configuration of the system (solid line). The temperature T is scaled by the mean-field steady-state temperature T_{MF} . The dash-dot line shows the time evolution of T according to Eq. (4). The nonequilibrium stationary temperature T_{NESS} is shown with dashed line. (b) The time evolution of fluctuation-induced force F scaled by T_{MF}/r_0 . (c) The probability distribution of F for the reference system where the simulation run over 10^8 time steps. The dashed line shows the best fit with a Gaussian distribution centered on $0.015T_{MF}r_0$.

average of F in the reference system equals to $\langle F \rangle_0 = 0.015T_{MF}/r_0$. The fluctuations are about two orders of magnitude larger than $\langle F \rangle_0$, thus very long simulations are required to measure the force with small numerical errors. Such a repulsive force between two intruder objects sitting at a distance larger than their radii was reported in the previous studies of driven granular gases [10, 12] and even dense shaken granular packings [28].

The time step length – that reflects the time scale for interaction with the heat bath – is chosen large enough that the dissipation is kept alive, but it is much smaller than the mean free time between the collisions. Since the energy considerations yield $\xi_0^2 = \sigma_0^2/(m^2\Delta t)$ [20], the steady state temperature (according to the Enskog theory) then becomes

$$T_{NESS} \propto \left(\frac{r \sigma^2}{\sqrt{m} \Delta t} \right)^{2/3}. \quad (4)$$

To investigate how the Casimir-like force is affected by the simulation parameters, we vary the parameter values one by one while the others are kept fixed at their reference values and measure the force. For this purpose, simulations are performed anew for each data point in Figs. 3(a-d) and the force is measured after the system reaches the steady state. We note that the values of $\langle F \rangle / \langle F \rangle_0$ around 5×10^{-2} reflect the accuracy level of our calculations. Therefore, the best fits with power-law functions (not shown in

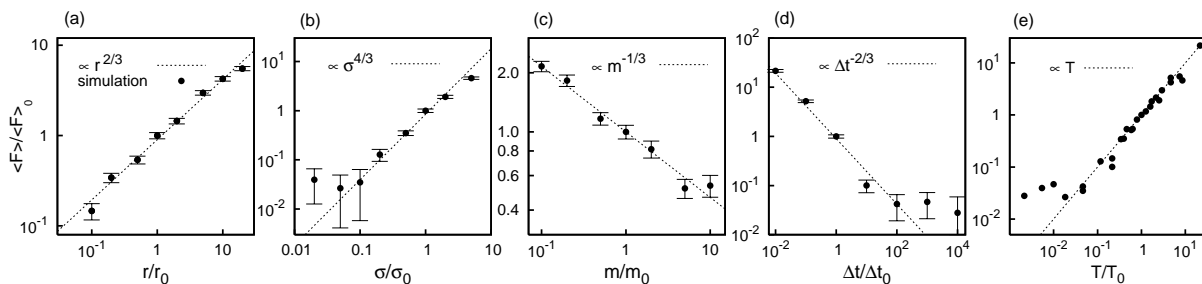


Figure 3. The fluctuation-induced force $\langle F \rangle$ scaled by $\langle F \rangle_0$ in terms of the grain radius r (a), the standard deviation of the momentum distribution σ (b), the grain mass m (c), and the time step Δt (d). The dashed lines are power-law functions with exponents correspond to those of Eq. (4). (e) $\langle F \rangle$ versus the temperature T . Here, the dashed line displays a linear growth of $\langle F \rangle$ with T .

Fig. 3) are obtained when the inaccurate data in Figs. 3(b) and (d) are neglected. Our results reveal that the exponents of the best fits approximately equal to the exponents of Eq. 4 with less than %6 errors. The stationary temperature is also measured for each data point in Figs. 3(a-d). The average force is plotted as a function of the temperature in Fig. 3(e) that interestingly verifies the linear dependence of the fluctuation-induced force on the temperature, as theoretically was predicted in the literature for the thermal fluctuating correlated media [2, 4].

Next we investigate how the effective interaction between the intruders is affected by the distance between them. Figure 4(a) displays that the average repulsive force $\langle F \rangle$ decays with increasing the distance D . Supposing a power-law dependence of $\langle F \rangle$ on D , one gets the exponent -0.8 ± 0.3 .

The repulsive force originates from the pressure difference between the hatched and cross-hatched regions in Fig. 1. The mechanism is briefly explained below (for details see [10]). In a system of hard disks, the pressure field p can be written as $p(n, T) = TH(n)$ [29], where n and T are fluctuating hydrodynamic fields. Expanding the pressure up to the second order around the stationary values (n_0, T_0) and taking its statistical average over the random noise source, we obtain $\langle p \rangle = p_0 + H_1 \langle \delta n \delta T \rangle + T_{MF} H_2 \langle \delta n^2 \rangle$, where p_0 is the stationary pressure and H_1 and H_2 are the first and second derivatives of $H(n)$ with respect to n around n_0 , respectively. By employing the Fourier transform of the fluctuating fields $\delta A(\mathbf{r}) = \sum_{\mathbf{k}} e^{-i\mathbf{k}\cdot\mathbf{r}} \delta A_{\mathbf{k}}/V$ and the structure factors $S_{AB}(\mathbf{k}) = \langle \delta A_{\mathbf{k}} \delta B_{-\mathbf{k}} \rangle/V$ [20] we rewrite p [10]:

$$\langle p \rangle = p_0 + V^{-1} \sum_{\mathbf{k}} [H_1 S_{nT}(\mathbf{k}) + T_{MF} H_2 S_{nn}(\mathbf{k})]. \quad (5)$$

In the calculation of the pressure the main contribution comes from the region of small \mathbf{k} . Substituting the structure factors of this region, $S_{AB}(\mathbf{k}) = S_{AB}^0/k^2$ (where S_{AB}^0 is a function of the number density, restitution coefficient and noise intensity), we obtain the steady-state pressure: $\langle p \rangle = p_0 + CV^{-1} \sum_{\mathbf{k}} (1/k^2)$, where $C = H_1 S_{nT}^0 + T_{MF} H_2 S_{nn}^0$ is a function of the number density n and is negative for our simulations. In the gap between the intruders, the number of valid k modes (and therefore $\sum_{\mathbf{k}} 1/k^2$) is smaller

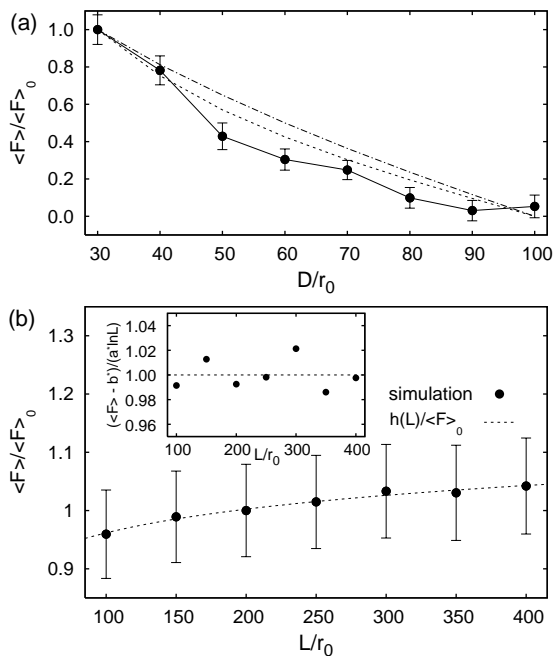


Figure 4. (a) The average force $\langle F \rangle$ scaled by $\langle F \rangle_0$ in terms of the distance between the intruders D scaled by r_0 . The dashed (dash-dot) line corresponds to the force calculation with (without) taking into account the actual boundary conditions. (b) $\langle F \rangle / \langle F \rangle_0$ as a function of the system size L . The dashed line corresponds to $h(L)$ scaled by $\langle F \rangle_0$. The inset shows how the deviation of the data from the logarithmic growth $h(L)$ varies with the system size.

than the outside region. Consequently, the pressure in the cross-hatched region is higher than the hatched region. This pressure difference Δp causes an effective repulsive force between the intruders. Interestingly, C (and therefore Δp and the fluctuation-induced force) is proportional to T_{MF} .

Δp is estimated in Ref. [10], supposing that k vectors are confined in rectangular boxes of size $(D - 2R) \times 2R$ and $(L - D - 2R) \times 2R$ in the gap between the intruders and in the outside region, respectively. The dash-dot line in Fig. 4(a) displays the Casimir force for different distances between the intruders, calculated according to the above mentioned estimation. The force is overestimated because (i) the geometrical simplification (using rectangular instead of circular boundary conditions) causes an error in the computed pressure, and (ii) the fluctuations are indeed correlated in the hatched and cross-hatched regions. We have improved this estimation by taking into account the circular shape of the intruders. At each point in the hatched or cross-hatched regions, the components of the allowed \mathbf{k} vectors in the x and y (perpendicular to x) directions are $(2\pi n_x/d_x(y), 2\pi n_y/L)$, where $d_x(y)$ is the length of the line segment that horizontally connects the surfaces of the two intruders. Using the continuous form of $\sum_k 1/k^2$, the pressure at this point reads

$$\langle p \rangle = p_0 + CV^{-1} \frac{(2\pi)^2}{Ld_x} \int_{2\pi/d_x}^{2\pi/r_0} dk_x \int_{2\pi/L}^{2\pi/r_0} dk_y \frac{1}{k_x^2 + k_y^2}, \quad (6)$$

Where an upper cutoff $2\pi/r_0$ is used beyond which hydrodynamics is not valid. This cutoff is also needed to exclude the singular vector $\mathbf{k} = (0, 0)$ from the integral. Calculating the pressure in the hatched and cross-hatched regions at a given y [according to Eq. (6)], we obtain $\Delta p(y)$. Next, by integrating $\Delta p(y)$ over the whole range of y ($-R, R$) to obtain the average force, and repeating the process for different distances between the intruders we get the dashed line in Fig. 4(a), revealing a significant improvement due to taking into account the actual boundary conditions. We note that the correlation between the fluctuations in the two regions seems to be important since our results still overestimate the force. One expects that the interaction between intruders would be affected if a new intruder is inserted into the system. Therefore, our results provides an important evidence for the nonlinearity of the Casimir-like forces in thermally noisy systems and offers new insight into the problem which should trigger new experiments and theoretical explanations.

Finally we study the system-size dependence of the effective force. It has been found in Ref. [20] that $T_{NESS} - T_{MF}$ in a two-dimensional driven granular gas is logarithmically divergent in the system size due to hydrodynamic fluctuations. Such a size dependence is also expected for $\langle F \rangle$ since we have verified a linear dependence of $\langle F \rangle$ on T_{NESS} . The simulation results [Fig. 4(b)] reveal that $\langle F \rangle$ increases slightly as the system size L increases and the data can be well fitted to a logarithmic curve $h(L) = a \ln L + b^*$ with less than %4 error. Within the investigated range of L , the deviation of the data from the logarithmic relation does not show a systematic dependence on the system size [inset of Fig. 4(b)]. The increase of $\langle F \rangle$ with L can be also explained qualitatively in the following way: When the system size is increased at a fixed D , the number of possible k modes (and $\sum_k 1/k^2$) in the hatched region of Fig. 1 increases; consequently, the mean pressure in the hatched region is reduced while the pressure in the cross-hatched region is not varied. This leads to the increase of pressure difference between the hatched and cross-hatched regions which yields the increase of $\langle F \rangle$.

4. Conclusions

In summary, we have carried out numerical simulations of the fluctuation-induced force between two intruders in a driven granular gas bed. Earlier works have demonstrated that such a force is expected since the thermodynamic properties are affected due to the presence of the intruders. Here, our main focus has been to study the fluctuating nature of this interaction and the temperature dependence of the ensemble average of the force $\langle F \rangle$. We have verified that $\langle F \rangle$ increases linearly with temperature, and slightly with system size that can be described by a logarithmic growth. We have also improved the estimation given in [10] to explain the force, by taking into account the actual boundary conditions of the problem.

5. Acknowledgments

We would like to express our gratitude to T. Unger for valuable discussions and B. Farnudi for reading the manuscript. J.S. acknowledges the Department of Physics of the Institute for Advanced Studies in Basic Sciences for the hospitality.

References

- [1] Casimir H. B. G., 1948 *Proc. K. Ned. Akad. Wet.* **51** 793
- [2] Kardar M. and Golestanian R., 1999 *Rev. Mod. Phys.* **71** 1233
- [3] Milonni P., 1994 *The Quantum Vacuum* (San Diego: Academic)
- [4] Krech M., 1994 *The Casimir Effect in Critical Systems* (Singapore: World Scientific)
- [5] Plunien G., Müller B. and Greiner W., 1986 *Phys. Rep.* **134** 87
Bordag M., Mohideen U. and Mostepanenko V. M., 2001 *Phys. Rep.* **353** 1
Milton K. A., 2004 *J. Phys. A: Math. Gen.* **37** R209
Lamoreaux S. K., 2005 *Rep. Prog. Phys.* **68** 201
Mostepanenko V. M. and Turnov N. N., 1997 *The Casimir Effect and its Applications* (Oxford: Clarendon)
Milton K. A., 2001 *The Casimir Effect: Physical Manifestations of the Zero-Point Energy* (Singapore: World Scientific)
- [6] Zihlerl P., Podgornik R. and Zumer S., 2000 *Phys. Rev. Lett.* **84** 1228
- [7] Fisher M. E. and de Gennes P. G., 1978 *C. R. Acad. Sci. Paris B* **287** 207
- [8] Hanke A. et al., 1998 *Phys. Rev. Lett.* **81** 1885
- [9] Ueno T. et al., 2003 *Phys. Rev. Lett.* **90** 116102
- [10] Cattuto C. et al., 2006 *Phys. Rev. Lett.* **96** 178001
- [11] Brito R., Marconi U. M. B. and Soto R., 2007 *Phys. Rev. E* **76** 011113
- [12] Brito R., Soto R. and Marconi U. M. B., 2007 *Granular Matter* **10** 29
- [13] Hertlein C. et al., 2008 *Nature* **451** 172
- [14] Kenneth O. et al., 2002 *Phys. Rev. Lett.* **89** 033001
- [15] Boyer T. H., 1974 *Phys. Rev. A* **9** 2078
- [16] Sanders D. A. et al., 2004 *Phys. Rev. Lett.* **93** 208002
- [17] Aumaitre S., Kruelle C. A. and Rehberg I., 2001 *Phys. Rev. E* **64** 041305
- [18] Zuriguel I. et al., 2005 *Phys. Rev. Lett.* **95** 258002
- [19] Jaeger H. M., Nagel S. R. and Behringer R. P., 1996 *Rev. Mod. Phys.* **68** 1259
- [20] van Noije T. P. C. et al., 1999 *Phys. Rev. E* **59** 4326
- [21] Peng G. and Ohta T., 1998 *Phys. Rev. E* **58** 4737
- [22] Du Y., Li H. and Kadanoff L. P., 1995 *Phys. Rev. Lett.* **74** 1268
- [23] van Noije T. P. C. et al., 1997 *Phys. Rev. Lett.* **79** 411
- [24] van Noije T. P. C., Ernst M. H. and Brito R., 1998 *Phys. Rev. E* **57** R4891
- [25] Chapman S. and Cowling T. G., 1970 *The Mathematical Theory of Non-uniform Gases* (Cambridge: Cambridge University Press)
- [26] Gradshteyn I. S. and Ryzhik I. M., 2007 *Table of Integrals, Series and Products* (Amsterdam: Academic Press) p 72
- [27] Bartolo D. et al., 2002 *Phys. Rev. Lett.* **89** 230601
- [28] Duran J. and Jullien R., 1998 *Phys. Rev. Lett.* **80** 3547
- [29] Verlet L. and Levesque D., 1982 *Mol. Phys.* **46** 969